Observational constraints on generalized Proca theories

Antonio De Felice[1], Lavinia Heisenberg[2], and Shinji Tsujikawa[3]
[1]*Center for Gravitational Physics, Yukawa Institute for Theoretical Physics, Kyoto University, 606-8502, Kyoto, Japan* [2]*Institute for Theoretical Studies, ETH Zurich, Clausiusstrasse 47, 8092 Zurich, Switzerland*
[3]*Department of Physics, Faculty of Science, Tokyo University of Science, 1-3, Kagurazaka, Shinjuku-ku, Tokyo 162-8601, Japan*
(Dated: March 11, 2022)

In a model of the late-time cosmic acceleration within the framework of generalized Proca theories, there exists a de Sitter attractor preceded by the dark energy equation of state $w_{\rm DE}=-1-s$, where s is a positive constant. We run the Markov-Chain-Monte-Carlo code to confront the model with the observational data of Cosmic Microwave Background (CMB), baryon acoustic oscillations, supernovae type Ia, and local measurements of the Hubble expansion rate for the background cosmological solutions and obtain the bound $s=0.254^{+0.118}_{-0.097}$ at 95 % confidence level (CL). Existence of the additional parameter s to those in the Λ-Cold-Dark-Matter (ΛCDM) model allows to reduce tensions of the Hubble constant H_0 between the CMB and the low-redshift measurements. Including the cosmic growth data of redshift-space distortions in the galaxy power spectrum and taking into account no-ghost and stability conditions of cosmological perturbations, we find that the bound on s is shifted to $s=0.16^{+0.08}_{-0.08}$ (95 % CL) and hence the model with $s>0$ is still favored over the ΛCDM model. Apart from the quantities s, H_0 and the today's matter density parameter Ω_{m0}, the constraints on other model parameters associated with perturbations are less stringent, reflecting the fact that there are different sets of parameters that give rise to a similar cosmic expansion and growth history.

arXiv:1703.09573v2 [astro-ph.CO] 24 Jun 2017

I. INTRODUCTION

Two fundamental pillars are used in the standard model of Big Bang cosmology for describing the physics on cosmological scales: the cosmological principle and General Relativity (GR). The first is the notion of homogeneity and isotropy. Even if the fundamental theory behind GR is very elegant and simple, the problems of cosmological constant and dark energy imply that we may need some modifications of GR in both infrared and ultraviolet scales. The cosmological constant problem represents the enormous discrepancy between observations and the expectations from a field theory point of view [1], whereas the dark energy problem stands for the observed late-time acceleration of the Universe. Another tenacious challenge is the successful construction of a consistent theory of quantum gravity. To address such problems, there have been numerous attempts for modifying gravity in the infrared and ultraviolet regimes [2–9].

In the context of infrared modifications of gravity, theories based on scalar fields are the most extensively explored ones. One essential reason for these considerations is the natural provision of isotropic accelerated expansion. Besides this practical reasoning, we know that scalar fields do exist in nature. The Higgs field is a fundamental ingredient of the Standard Model of particle physics. Accepting an additional scalar degree of freedom in the gravity sector, the scalar field has to be very light to drive the late-time cosmic acceleration. This new scalar degree of freedom generally gives rise to long-range forces with baryonic matter, but such fifth forces have never been detected in solar-system tests of gravity [10]. Therefore, one has to rely on some successful implementations of screening mechanisms, which hide the scalar field on small scales whereas being unleashed on large scales to produce desired cosmological effects. In particular, the Vainshtein mechanism [11] in the presence of non-linear field self-interactions can efficiently screen the propagation of fifth forces within a radius much larger than the solar-system scale [12–17].

An interesting class of the self-interacting scalar field with a Galileon symmetry was proposed in Ref. [18]. These Galileon interactions involve explicit dependence on second derivatives of the scalar field in their Lagrangians, but they maintain the second-order nature of field equations such that the Ostrogradski instability is avoided. A naive covariantization of these Galileon interactions would result in higher-order equations of motion. This can be prevented by including corresponding non-minimal derivative couplings with the Ricci scalar and the Einstein tensor [19, 20]. The generalization of covariant Galileons led to the construction of theories respecting the Galilean symmetry on the de Sitter background [21] and the rediscovery of the Horndeski action [22].

Horndeski theories constitute the most general scalar-tensor theories leading to second-order equations of motion with one scalar propagating degree of freedom besides two tensor polarizations [22–25]. Similar scalar-tensor theories with second-order equations of motion also arise from the decoupling limit of massive gravity [26–29]. Even outside the second-order domain, it is possible to construct more general scalar-tensor theories with one scalar propagating degree of freedom [30–32]. All these new realms of possibilities have been giving rise to a plethora of attempts for

describing dark energy. These attempts also shed light to how classical field theories can be constructed in a consistent way as to keep the theory sensible and viable, i.e., without introducing ghost instabilities and removing unwanted degrees of freedom.

The Standard Model of particle physics contains both abelian and non-abelian vector fields as the fundamental carriers of gauge interactions. Consequently, it is comprehensible to wonder whether bosonic vector fields may also play an important role in the cosmological evolution besides scalar fields. Similarly to the scalar counterpart, vector fields being part of the gravitational interactions could naturally result in an accelerated Universe on large scales while being screened on small scales. Learned from the lessons for constructing consistent theories for scalar-tensor interactions, one can apply the same approach to vector-tensor theories. In Minkowski space-time, allowing for a mass of the vector field leads to the propagation of a longitudinal scalar mode besides two transverse vector polarizations due to the breaking of $U(1)$ gauge invariance. One can generalize this massive Proca theory to that in curved space-time in such a way that the propagating degrees of freedom remain three besides two tensor polarizations. A specific type of massive Proca theories naturally arise in the framework of Weyl geometries [33, 34].

The generalized Proca theories with second-order equations of motion constitute Galileon type vector self-interactions with non-minimal derivative couplings to gravity. The systematic construction of the action of generalized Proca theories was carried out in Ref. [35], where it was shown that despite the derivative self-interactions only three physical degrees of freedom propagate. The specific case where the longitudinal mode of the vector field has the scalar Galilean self-interactions was considered in Ref. [36]. These generalized Proca interactions were further investigated in Refs. [37, 38]. Even outside the domain of second-order theories, one can construct more general vector-tensor interactions without increasing the number of propagating degrees of freedom relative to that in generalized Proca theories [39, 40].

Recently, the background cosmological solutions and the stabilities of perturbations were studied for concrete dark energy models that belong to generalized Proca theories [41, 42]. These models can be also compatible with solar-system constraints for a wide range of parameter space [43]. At the background level, there exists a de Sitter attractor responsible for the late-time cosmic acceleration. Moreover, it was illustrated how dark energy models in the framework of generalized Proca theories can be observationally distinguished from the standard cosmological model according to both expansion history and cosmic growth [41, 42]. Within this framework of generalized Proca interactions, the de Sitter solution arises from the temporal component of the vector field compatible with the symmetries of homogeneity and isotropy of the Friedmann-Lemaître-Robertson-Walker (FLRW) background. Even if the temporal component does not correspond to a propagating degree of freedom by construction, it does have a non-trivial effect on the cosmological dynamics by behaving as an auxiliary field. Another way of constructing homogeneous and isotropic cosmological solutions within this class of theories consists of considering triads configuration [44, 45]. A third possibility is a combination of the temporal configuration with the triads as proposed in Ref. [44]. It would be worthwhile to investigate the cosmological implications of this type of multi-Proca interactions and extend the existing studies [44, 46–50].

In this work, we go along the lines of Refs. [41, 42] and place constraints on these models by using several different cosmological data sets: the Cosmic Microwave Background (CMB) shift parameters (from the Planck data), Baryon Acoustic Oscillations (BAO), Supernova Type Ia (SN Ia) standard candles (from the Union 2.1 data), local measurements of the Hubble expansion rate, and Redshift-Space-Distortions (RSD). The Λ-Cold-Dark-Matter (ΛCDM) model requires typical values of today's density parameter of non-relativistic matter Ω_{m0} to be around 0.31, whereas, in generalized Proca theories, smaller values of Ω_{m0} are reached due to the existence of an extra parameter, s. Moreover, the Hubble constant H_0 tends to be higher in generalized Proca theories with a lower total χ^2 relative to that in the ΛCDM model. Therefore, generalized Proca theories can help to reduce the tension between early-time and late-time data sets, compared to the ΛCDM model.

This paper is organized as follows. In Sec. II we review the background cosmological dynamics for a class of dark energy models in the framework of generalized Proca theories. In Sec. III we discuss stability conditions and the evolution of matter density perturbations relevant to the growth of large-scale structures. In Sec. IV we explain the data sets used for the likelihood analysis in later sections. In Sec. V we place observational bounds on model parameters associated with the background expansion history by using the data of CMB, BAO, SN Ia, and Hubble expansion rate. In Sec. VI we put constraints on model parameters related to linear cosmological perturbations by adding the RSD data in the analysis. Sec. VII is devoted to conclusions.

II. GENERALIZED PROCA THEORIES AND THE BACKGROUND DYNAMICS

In generalized Proca theories, the vector field A^μ possesses two transverse polarizations and one longitudinal scalar mode non-minimally coupled to gravity. To keep the equations of motion up to second order, the field self-interactions

need to be of specific forms. The action of generalized Proca theories is given by [35, 38]

$$S = \int d^4x\sqrt{-g}\,(\mathcal{L}+\mathcal{L}_M)\,, \qquad \mathcal{L} = \sum_{i=2}^{6}\mathcal{L}_i\,, \tag{2.1}$$

where g is the determinant of the metric tensor $g_{\mu\nu}$, $\mathcal{L}_M$ is the matter Lagrangian density, and $\mathcal{L}_{2,3,4,5,6}$ are the vector-tensor interactions given by

$$\mathcal{L}_2 = G_2(X,F,Y)\,, \tag{2.2}$$

$$\mathcal{L}_3 = G_3(X)\nabla_\mu A^\mu\,, \tag{2.3}$$

$$\mathcal{L}_4 = G_4(X)R + G_{4,X}(X)\left[(\nabla_\mu A^\mu)^2 - \nabla_\rho A_\sigma \nabla^\sigma A^\rho\right]\,, \tag{2.4}$$

$$\mathcal{L}_5 = G_5(X)G_{\mu\nu}\nabla^\mu A^\nu - \frac{1}{6}G_{5,X}(X)[(\nabla_\mu A^\mu)^3 - 3\nabla_\mu A^\mu \nabla_\rho A_\sigma \nabla^\sigma A^\rho + 2\nabla_\rho A_\sigma \nabla^\gamma A^\rho \nabla^\sigma A_\gamma] - g_5(X)\tilde{F}^{\alpha\mu}\tilde{F}^{\beta}{}_{\mu}\nabla_\alpha A_\beta\,, \tag{2.5}$$

$$\mathcal{L}_6 = G_6(X)L^{\mu\nu\alpha\beta}\nabla_\mu A_\nu \nabla_\alpha A_\beta + \frac{1}{2}G_{6,X}(X)\tilde{F}^{\alpha\beta}\tilde{F}^{\mu\nu}\nabla_\alpha A_\mu \nabla_\beta A_\nu\,. \tag{2.6}$$

The field strength is $F_{\mu\nu} = \nabla_\mu A_\nu - \nabla_\nu A_\mu$ and its dual is $\tilde{F}^{\mu\nu} = \epsilon^{\mu\nu\alpha\beta}F_{\alpha\beta}/2$, where ∇_μ stands for the covariant derivative operator. The function G_2 can depend in general on the quantities

$$X = -\frac{1}{2}A_\mu A^\mu\,, \qquad F = -\frac{1}{4}F_{\mu\nu}F^{\mu\nu}\,, \qquad Y = A^\mu A^\nu F_\mu{}^\alpha F_{\nu\alpha}\,, \tag{2.7}$$

while the remaining functions $G_{3,4,5,6}$ and g_5 depend only on X. The partial derivatives of the functions are denoted by $G_{i,X} \equiv \partial G_i/\partial X$. In the same way as in scalar Horndeski theories, the vector field is coupled only to the divergenceless tensors and their corresponding versions at the level of the equations of motion. Hence, the vector field is directly coupled to the Ricci scalar R, the Einstein tensor $G_{\mu\nu} = R_{\mu\nu} - Rg_{\mu\nu}/2$, and the double dual Riemann tensor

$$L^{\mu\nu\alpha\beta} = \frac{1}{4}\epsilon^{\mu\nu\rho\sigma}\epsilon^{\alpha\beta\gamma\delta}R_{\rho\sigma\gamma\delta}\,, \tag{2.8}$$

where $\epsilon^{\mu\nu\rho\sigma}$ is the Levi-Civita tensor and $R_{\rho\sigma\gamma\delta}$ is the Riemann tensor. The specific case with $G_2 = m^2X$ and $G_{3,4,5,6} = 0$ corresponds to the standard Proca theory, in which case two transverse vector modes and the longitudinal scalar propagate. These three propagating degrees of freedom are not altered by the derivative interactions (2.2)-(2.6), apart from the appearance of two tensor polarizations from the gravity sector [35, 40]. The non-minimal derivative couplings (2.4)-(2.6) are needed to keep the equations of motion up to second order. The gauge-invariant vector-tensor interaction introduced by Horndeski in 1976 corresponds to $\mathcal{L} = F + \mathcal{L}_4 + \mathcal{L}_6$ with constant functions G_4 and G_6 [51].

A. Background equations of motion

For the purpose of cosmological applications, we take the flat FLRW metric with the line element $ds^2 = -dt^2 + a^2(t)\delta_{ij}dx^i dx^j$, where $a(t)$ stands for the time-dependent scale factor with the cosmic time t. We consider the vector field A^μ with a time-dependent temporal component $\phi(t)$ alone, i.e.,

$$A^\mu = (\phi(t), 0, 0, 0)\,, \tag{2.9}$$

which is compatible with the background symmetry. Assuming that the matter field in the Lagrangian density $\mathcal{L}_M$ (with energy density ρ_M and pressure P_M) is minimally coupled to gravity, they obey the continuity equation

$$\dot{\rho}_M + 3H(\rho_M + P_M) = 0\,, \tag{2.10}$$

where $H \equiv \dot{a}/a$ is the Hubble expansion rate, and a dot represents a derivative with respect to t. Varying the action (2.1) with respect to $g_{\mu\nu}$, we obtain the modified Einstein field equations

$$G_2 - G_{2,X}\phi^2 - 3G_{3,X}H\phi^3 + 6G_4H^2 - 6(2G_{4,X} + G_{4,XX}\phi^2)H^2\phi^2 + G_{5,XX}H^3\phi^5 + 5G_{5,X}H^3\phi^3 = \rho_M\,, \tag{2.11}$$

$$G_2 - \dot{\phi}\phi^2 G_{3,X} + 2G_4\,(3H^2 + 2\dot{H}) - 2G_{4,X}\phi\,(3H^2\phi + 2H\dot{\phi} + 2\dot{H}\phi) - 4G_{4,XX}H\dot{\phi}\phi^3 + G_{5,XX}H^2\dot{\phi}\phi^4 + G_{5,X}H\phi^2(2\dot{H}\phi + 2H^2\phi + 3H\dot{\phi}) = -P_M\,. \tag{2.12}$$

Variation of the action (2.1) with respect to ϕ leads to

$$\phi \left(G_{2,X} + 3G_{3,X} H\phi + 6G_{4,X} H^2 + 6G_{4,XX} H^2 \phi^2 - 3G_{5,X} H^3 \phi - G_{5,XX} H^3 \phi^3 \right) = 0 \,. \tag{2.13}$$

The functions g_5, G_6 and the additional dependence of F and Y in the function G_2, which correspond to intrinsic vector modes, do not contribute to the background equations of motion as expected. From Eq. (2.13) one immediately observes that, for the branch $\phi \neq 0$, there exist interesting de Sitter solutions with constant values of ϕ and H [41].

B. Concrete models

In a previous work, we have shown that viable dark energy models exist in the framework of generalized Proca theories [41]. As we mentioned before, the temporal vector component is not dynamical and can be expressed in terms of the Hubble parameter H. In order for the energy density of the temporal component ϕ to start dominating over the background matter densities at the late cosmological epoch, the amplitude of the field ϕ should increase with the decrease of H. Thus, the relation should be of the form

$$\phi^p \propto H^{-1} \,, \tag{2.14}$$

with a positive constant p. In the following, we assume that ϕ is positive. To guarantee the scaling (2.14) between ϕ and H, the functions $G_{2,3,4,5}$ in Eq. (2.13) should be chosen with the following specific scaling of X [41]:

$$G_2(X) = b_2 X^{p_2} + F \,, \qquad G_3(X) = b_3 X^{p_3} \,, \qquad G_4(X) = \frac{M_{\rm pl}^2}{2} + b_4 X^{p_4} \,, \qquad G_5(X) = b_5 X^{p_5} \,, \tag{2.15}$$

with the powers $p_{3,4,5}$ of the form

$$p_3 = \frac{1}{2}\left(p + 2p_2 - 1\right) \,, \qquad p_4 = p + p_2 \,, \qquad p_5 = \frac{1}{2}\left(3p + 2p_2 - 1\right) \,, \tag{2.16}$$

where $M_{\rm pl}$ is the reduced Planck mass and $b_{2,3,4,5}$ are constants. Note that the specific case with $p_2 = 1$ and $p = 1$ corresponds to vector Galileons [35, 36], where $\phi \propto H^{-1}$. The models given by the functions (2.15) are the generalization of vector Galileons.

For the matter fields, we will assume the existence of non-relativistic matter (energy density ρ_m and pressure $P_m = 0$) and radiation (energy density ρ_r and pressure $P_r = \rho_r/3$) together with their respective continuity equations $\dot{\rho}_m + 3H\rho_m = 0$ and $\dot{\rho}_r + 4H\rho_r = 0$. Then we have $\rho_M = \rho_m + \rho_r$ and $P_M = \rho_r/3$ in Eqs. (2.11) and (2.12), respectively. For later convenience, we define the following dimensionless quantities (where $i = 3, 4, 5$):

$$y \equiv \frac{b_2 \phi^{2p_2}}{3M_{\rm pl}^2 H^2\, 2^{p_2}} \,, \qquad \beta_i \equiv \frac{p_i b_i}{2^{p_i - p_2} p_2 b_2} \left(\phi^p H\right)^{i-2} \,, \tag{2.17}$$

and the density parameters

$$\Omega_r \equiv \frac{\rho_r}{3M_{\rm pl}^2 H^2} \,, \qquad \Omega_m \equiv \frac{\rho_m}{3M_{\rm pl}^2 H^2} \,, \qquad \Omega_{\rm DE} \equiv 1 - \Omega_r - \Omega_m \,. \tag{2.18}$$

The variables β_i's are constants due to the relation (2.14). For the branch $\phi \neq 0$, Eq. (2.13) is expressed in a simple form

$$1 + 3\beta_3 + 6(2p + 2p_2 - 1)\beta_4 - (3p + 2p_2)\beta_5 = 0 \,, \tag{2.19}$$

which can be exploited to express β_3 in terms of β_4 and β_5. On using Eq. (2.11), the dark energy density parameter is related to the quantity y, as

$$\Omega_{\rm DE} = \frac{\beta y}{p_2(p + p_2)} \,, \tag{2.20}$$

where the constant β is defined by

$$\beta \equiv -p_2(p + p_2)(1 + 4p_2\beta_5) + 6p_2^2(2p + 2p_2 - 1)\beta_4 \,. \tag{2.21}$$

For the constant b_2 appearing in $G_2(X)$, we choose it to be negative, i.e., $b_2 = -m^2 M_{\rm pl}^{2(1-p_2)}$, where m is a mass term. This is for avoiding the appearance of tensor ghosts in the limit that $G_5 \to 0$ [41]. We also introduce the following dimensionless quantity

$$\lambda \equiv \left(\frac{\phi}{M_{\rm pl}}\right)^p \frac{H}{m}\,, \tag{2.22}$$

which is constant from Eq. (2.14). On using Eqs. (2.17) and (2.21), the temporal vector component can be expressed as $\phi = M_{\rm pl}[-2^{p_2}\cdot 3\lambda^2 p_2(p+p_2)\Omega_{\rm DE}/\beta]^{1/[2(p+p_2)]}$. We will focus on the case $\beta < 0$, under which $\phi > 0$ and $\lambda > 0$ for $p_2(p+p_2) > 0$.

To bring the equations of motion into an autonomous form, we perform the following manipulations: first we differentiate the $\phi \neq 0$ branch of Eq. (2.13) with respect to t and together with Eq. (2.12) we can solve them for $\dot{\phi}$ and $\dot{H}$. Taking the derivatives of $\Omega_{\rm DE}$ and Ω_r with respect to $\mathcal{N} \equiv \ln a$ (denoted by a prime), we obtain the following autonomous equations

$$\Omega'_{\rm DE} = \frac{(1+s)\Omega_{\rm DE}(3+\Omega_r-3\Omega_{\rm DE})}{1+s\,\Omega_{\rm DE}}\,, \tag{2.23}$$

$$\Omega'_r = -\frac{\Omega_r[1-\Omega_r+(3+4s)\Omega_{\rm DE}]}{1+s\,\Omega_{\rm DE}}\,, \tag{2.24}$$

where we introduced the variable

$$s \equiv \frac{p_2}{p}\,. \tag{2.25}$$

After integrating Eqs. (2.23) and (2.24) for given initial conditions of $\Omega_{\rm DE}$ and Ω_r, the three density parameters $\Omega_{\rm DE}, \Omega_r$ and $\Omega_m = 1-\Omega_{\rm DE}-\Omega_r$ are known accordingly. Furthermore, we impose the condition $s > -1$ to prevent $\Omega_{\rm DE}$ from diverging in the interval $0 \le \Omega_{\rm DE} \le 1$. We also define the effective equation of state of the system by $w_{\rm eff} \equiv -1 - 2\dot{H}/(3H^2)$, which can be expressed as

$$w_{\rm eff} = \frac{\Omega_r - 3(1+s)\Omega_{\rm DE}}{3(1+s\,\Omega_{\rm DE})}\,. \tag{2.26}$$

We write Eqs. (2.11) and (2.12) in the forms $3M_{\rm pl}^2H^2 = \rho_{\rm DE}+\rho_M$ and $M_{\rm pl}^2(3H^2+2\dot{H}) = -P_{\rm DE}-P_M$, respectively, where

$$\rho_{\rm DE} = -G_2 + G_{2,X}\phi^2 + 3G_{3,X}\phi^3 H - 6g_4H^2 + 6\phi^2H^2(2G_{4,X}+G_{4,XX}\phi^2) - H^3G_{5,XX}\phi^5 - 5H^3G_{5,X}\phi^3, \tag{2.27}$$

$$\begin{aligned} P_{\rm DE} &= G_2 - \dot{\phi}\phi^2 G_{3,X} + 2g_4\,(3H^2+2\dot{H}) - 2\phi G_{4,X}\,(3\phi H^2 + 2\dot{\phi}H + 2\phi\dot{H}) \\ &\quad - 4H\dot{\phi}\phi^3 G_{4,XX} + \dot{\phi}\phi^4 H^2 G_{5,XX} + G_{5,X}\phi^2 H(2\phi\dot{H} + 2\phi H^2 + 3\dot{\phi}H)\,, \end{aligned} \tag{2.28}$$

with $g_4(X) = b_4X^{p_4}$. Defining the dark energy equation of state as $w_{\rm DE} = P_{\rm DE}/\rho_{\rm DE}$, it follows that

$$w_{\rm DE} = -\frac{3(1+s)+s\,\Omega_r}{3(1+s\,\Omega_{\rm DE})}\,. \tag{2.29}$$

Using Eqs. (2.23) and (2.24), we obtain a single differential equation of the form

$$\frac{\Omega'_{\rm DE}}{\Omega_{\rm DE}} = (1+s)\left(\frac{\Omega'_r}{\Omega_r}+4\right)\,. \tag{2.30}$$

This equation is easily integrated to give

$$\frac{\Omega_{\rm DE}}{\Omega_r^{1+s}} = \frac{\Omega_{\rm DE0}}{\Omega_{r0}^{1+s}}\left(\frac{a}{a_0}\right)^{4(1+s)}\,, \tag{2.31}$$

where the lower subscript "0" denotes today's values.

III. COSMOLOGICAL PERTURBATIONS

By considering linear cosmological perturbations on the flat FLRW background, the conditions for avoiding ghosts and Laplacian instabilities in the small-scale limit were already derived in Refs. [41, 42]. Here, we briefly review six no-ghost and stability conditions arising from tensor, vector, and scalar perturbations. We also discuss the equations of motion for matter perturbations to confront generalized Proca theories with the observations of RSD in Sec. VI.

A. Stability conditions

For the metric we take the perturbed line element in the flat gauge

$$ds^2 = -(1+2\alpha)\,dt^2 + 2\,(\partial_i\chi + V_i)\,dt\,dx^i + a^2(t)\,(\delta_{ij} + h_{ij})\,dx^i dx^j\,, \tag{3.1}$$

where α, χ are scalar metric perturbations, V_i is the vector perturbation obeying the transverse condition $\partial^i V_i = 0$, and h_{ij} is the tensor perturbation satisfying the transverse and traceless conditions $\partial^i h_{ij} = 0$ and $h_i{}^i = 0$. The temporal and spatial components of the vector field can be decomposed into the background and perturbed parts, as

$$A^0 = \phi(t) + \delta\phi\,, \qquad A^i = \frac{1}{a^2(t)}\delta^{ij}\,(\partial_j\chi_V + E_j)\,, \tag{3.2}$$

where $\delta\phi$ and χ_V are scalar perturbations, and E_j is the vector perturbation satisfying $\partial^j E_j = 0$. The Schutz-Sorkin action [52] allows us to describe both vector and scalar perturbations of the matter perfect fluid. For scalar perturbations, the key observables are the matter density perturbation $\delta\rho_M$ and the velocity potential v.

First of all, the tensor perturbation h_{ij} has two polarization modes h_+ and $h_\times$, which can be expressed as $h_{ij} = h_+ e^+_{ij} + h_\times e^\times_{ij}$ in terms of the unit tensors obeying the normalizations $e^+_{ij}(\boldsymbol{k})e^+_{ij}(-\boldsymbol{k})^* = 1$, $e^\times_{ij}(\boldsymbol{k})e^\times_{ij}(-\boldsymbol{k})^* = 1$, $e^+_{ij}(\boldsymbol{k})e^\times_{ij}(-\boldsymbol{k})^* = 0$. Expanding the action (2.1) in h_{ij} up to quadratic order, the second-order action yields

$$S_T = \sum_{\lambda=+,\times}\int dt\,d^3x\,a^3\,\frac{q_T}{8}\left[\dot{h}_\lambda^2 - \frac{c_T^2}{a^2}(\partial h_\lambda)^2\right]. \tag{3.3}$$

The quantities q_T and c_T^2 determine no-ghost and stability conditions, respectively, whose explicit forms are given by

$$q_T = 2G_4 - 2\phi^2 G_{4,X} + H\phi^3 G_{5,X} > 0\,, \tag{3.4}$$

$$c_T^2 = \frac{2G_4 + \phi^2\dot{\phi}\,G_{5,X}}{q_T} > 0\,. \tag{3.5}$$

For vector perturbations, the dynamical field is given by the combination

$$Z_i = E_i + \phi(t)V_i\,. \tag{3.6}$$

Due to the transverse condition $\partial^i Z_i = 0$, there are two propagating degrees of freedom for Z_i, e.g., $Z_i = (Z_1(z), Z_2(z), 0)$ for the vector field whose wavenumber $\boldsymbol{k}$ is along the z direction. Expanding the action (2.1) up to quadratic order and taking the small-scale limit, the resulting second-order action for Z_1 and Z_2 can be written as the form analogous to Eq. (3.3) with the no-ghost and stability conditions

$$q_V = G_{2,F} + 2G_{2,Y}\phi^2 - 4g_5 H\phi + 2G_6 H^2 + 2G_{6,X}H^2\phi^2 > 0\,, \tag{3.7}$$

$$c_V^2 = 1 + \frac{\phi^2(2G_{4,X} - G_{5,X}H\phi)^2}{2q_T q_V} + \frac{2[G_6\dot{H} - G_{2,Y}\phi^2 - (H\phi - \dot{\phi})(H\phi\,G_{6,X} - g_5)]}{q_V} > 0\,. \tag{3.8}$$

For scalar perturbations, the dynamical field arising from the vector field is given by

$$\psi = \chi_V + \phi(t)\chi\,. \tag{3.9}$$

The matter perturbation $\delta\rho_M$, which arises from the Schutz-Sorkin action, also works as a dynamical scalar field. The second-order action of scalar perturbations is given in Eq. (4.6) of Ref. [42]. Varying this action with respect to $\alpha, \chi, \delta\phi, \partial\psi, v$, and $\delta\rho_M$, the equations of motion in Fourier space are given, respectively, by

$$\delta\rho_M - 2w_4\alpha + (3Hw_1 - 2w_4)\frac{\delta\phi}{\phi} + \frac{k^2}{a^2}(\mathcal{Y} + w_1\chi - w_6\psi) = 0\,, \tag{3.10}$$

$$(\rho_M + P_M)\,v + w_1\alpha + \frac{w_2}{\phi}\delta\phi = 0\,, \tag{3.11}$$

$$(3Hw_1 - 2w_4)\,\alpha - 2w_5\frac{\delta\phi}{\phi} + \frac{k^2}{a^2}\left[\frac{1}{2}\mathcal{Y} + w_2\chi - \frac{1}{2}\left(\frac{w_2}{\phi} + w_6\right)\psi\right] = 0\,, \tag{3.12}$$

$$\dot{\mathcal{Y}} + \left(H - \frac{\dot{\phi}}{\phi}\right)\mathcal{Y} + 2\phi\,(w_6\alpha + w_7\psi) + \left(\frac{w_2}{\phi} + w_6\right)\delta\phi = 0\,, \tag{3.13}$$

$$\dot{\delta\rho}_M + 3H\left(1 + c_M^2\right)\delta\rho_M + \frac{k^2}{a^2}(\rho_M + P_M)(\chi + v) = 0\,, \tag{3.14}$$

$$\dot{v} - 3Hc_M^2 v - c_M^2\frac{\delta\rho_M}{\rho_M + P_M} - \alpha = 0\,, \tag{3.15}$$

where c_M^2 is the matter propagation speed squared, and

$$w_1 = H^2\phi^3(G_{5,X}+\phi^2 G_{5,XX}) - 4\,H(G_4+\phi^4 G_{4,XX}) - \phi^3 G_{3,X}\,, \tag{3.16}$$
$$w_2 = w_1 + 2Hq_T\,, \tag{3.17}$$
$$w_3 = -2\phi^2 q_V\,, \tag{3.18}$$
$$w_4 = \frac{1}{2}H^3\phi^3(9G_{5,X}-\phi^4 G_{5,XXX}) - 3\,H^2(2G_4+2\phi^2 G_{4,X}+\phi^4 G_{4,XX}-\phi^6 G_{4,XXX}) \\ -\frac{3}{2}\,H\phi^3(G_{3,X}-\phi^2 G_{3,XX}) + \frac{1}{2}\,\phi^4 G_{2,XX}\,, \tag{3.19}$$
$$w_5 = w_4 - \frac{3}{2}\,H(w_1+w_2)\,, \tag{3.20}$$
$$w_6 = -\phi\left[H^2\phi(G_{5,X}-\phi^2 G_{5,XX}) - 4\,H(G_{4,X}-\phi^2 G_{4,XX}) + \phi G_{3,X}\right]\,, \tag{3.21}$$
$$w_7 = 2(H\phi G_{5,X}-2G_{4,X})\dot{H} + \left[H^2(G_{5,X}+\phi^2 G_{5,XX}) - 4\,H\phi\,G_{4,XX} - G_{3,X}\right]\dot{\phi}\,, \tag{3.22}$$
$$\mathcal{Y} = \frac{w_3}{\phi}\left(\dot{\psi}+\delta\phi+2\alpha\phi\right)\,. \tag{3.23}$$

On using Eqs. (3.10)-(3.12) and (3.14), we can express $\alpha, \chi, \delta\phi, v$ in terms of $\psi, \delta\rho_M$ and their derivatives. Then, the second-order action of scalar perturbations is written in terms of the two dynamical fields ψ and $\delta\rho_M$. This allows one to derive no-ghost and stability conditions in the small-scale limit. The no-ghost and stability conditions of the matter field $\delta\rho_M$ are trivially satisfied for $\rho_M + P_M > 0$ and $c_M^2 > 0$. For the perturbation ψ, we require the following conditions [41, 42]

$$Q_S = \frac{a^3 H^2 q_T q_S}{\phi^2(w_1-2w_2)^2} > 0\,, \tag{3.24}$$
$$c_S^2 = \frac{\mu_S}{8H^2\phi^2 q_T q_V q_S} > 0\,, \tag{3.25}$$

where

$$q_S = 3w_1^2 + 4q_T w_4\,, \tag{3.26}$$
$$\mu_S = \left[w_6\phi(w_1-2w_2)+w_1 w_2\right]^2 - w_3\left(2w_2^2\dot{w}_1 - w_1^2\dot{w}_2\right) + \phi\,(w_1-2w_2)^2\,w_3\dot{w}_6 \\ +w_3(w_1-2w_2)\left[\left(H-2\dot{\phi}/\phi\right)w_1 w_2 + (w_1-2w_2)\left\{w_6\left(H\phi-\dot{\phi}\right)+2w_7\phi^2\right\}\right] \\ +2w_2^2 w_3\,(\rho_M+P_M)\,. \tag{3.27}$$

Under the no-ghost conditions of tensor and vector perturbations ($q_T > 0, q_V > 0$), Eqs. (3.24) and (3.25) can be satisfied for $q_S > 0$ and $\mu_S > 0$. There are specific cases where the quantity $w_1 - 2w_2$ in Eq. (3.24) crosses 0, at which Q_S exhibits the divergence [41]. We will exclude such cases for constraining the viable parameter space.

B. Effective gravitational coupling with matter perturbations

To confront generalized Proca theories with the observations of large-scale structures and weak lensing, we consider non-relativistic matter (labeled by m) with the equation of state $w_m = P_m/\rho_m = 0^+$ and the sound speed squared $c_m^2 = 0^+$. We introduce the matter density contrast δ and the gauge-invariant gravitational potentials

$$\delta = \frac{\delta\rho_m}{\rho_m} + 3Hv\,, \qquad \Psi = \alpha + \dot{\chi}\,, \qquad \Phi = H\chi\,. \tag{3.28}$$

Taking the time derivative of Eq. (3.14) and using Eq. (3.15), we obtain

$$\ddot{\delta} + 2H\dot{\delta} + \frac{k^2}{a^2}\Psi = 3\ddot{\mathcal{B}} + 6H\dot{\mathcal{B}}\,, \tag{3.29}$$

where $\mathcal{B} \equiv Hv$. The effective gravitational coupling $G_{\rm eff}$ is defined by

$$\frac{k^2}{a^2}\Psi = -4\pi G_{\rm eff}\rho_m\delta\,. \tag{3.30}$$

For the perturbations deep inside the sound horizon ($c_S^2k^2/a^2 \gg H^2$), we can resort to the quasi-static approximation for deriving the relations between Ψ, Φ and δ [53–55]. Provided that c_S^2 is not very much smaller than 1, the dominant contributions to the perturbation equations of motion are the terms containing k^2/a^2 and $\delta\rho_m$. The terms on the r.h.s. of Eq. (3.29) are negligible relative to those on the l.h.s., so that

$$\ddot{\delta} + 2H\dot{\delta} - 4\pi G_{\rm eff}\rho_m\delta \simeq 0\,. \tag{3.31}$$

On using the quasi-static approximation for Eqs. (3.10)-(3.13), the effective gravitational coupling is analytically known as [42]

$$G_{\rm eff} = \frac{\xi_2+\xi_3}{\xi_1}\,, \tag{3.32}$$

where

$$\xi_1 = 4\pi\phi^2\left(w_2+2Hq_T\right)^2\,, \tag{3.33}$$

$$\xi_2 = \left[H\left(w_2+2Hq_T\right) - \dot{w}_1 + 2\dot{w}_2 + \rho_m\right]\phi^2 - \frac{w_2^2}{q_V}\,, \tag{3.34}$$

$$\xi_3 = \frac{1}{8H^2\phi^2q_S^3q_Tc_S^2}\Big[2\phi^2\left\{q_S[w_2\dot{w}_1 - (w_2-2Hq_T)\dot{w}_2] + \rho_m w_2[3w_2(w_2+2Hq_T) - q_S]\right\} + \frac{q_S}{q_V}w_2\left\{w_2(w_2-2Hq_T) - w_6\phi(w_2+2Hq_T)\right\}\Big]^2\,. \tag{3.35}$$

The solutions to δ derived by solving Eq. (3.31) with Eq. (3.32) can reproduce full numerical results at high accuracy [42].

Besides $G_{\rm eff}$, the gravitational slip parameter $\eta = -\Phi/\Psi$ is also an important quantity for describing the deviation of light rays in weak lensing observations [56]. Under the quasi-static approximation it follows that [42]

$$\eta = \frac{\xi_4}{\xi_2+\xi_3}\,, \tag{3.36}$$

where

$$\xi_4 = \frac{w_2+2Hq_T}{4Hq_S^2q_Vq_Tc_S^2}\Big[4H^2\phi^2q_S^2q_Vq_Tc_S^2 + 2\phi^2q_Sq_Vw_2\dot{w}_2(w_2-2Hq_T) + w_2^2\{\phi q_Sw_6(w_2+2Hq_T) - w_2q_S(w_2-2Hq_T) - 2\phi^2q_Sq_V\dot{w}_1 + 2\phi^2q_V[q_S-3w_2(w_2+2Hq_T)]\rho_m\}\Big]\,. \tag{3.37}$$

Although we do not use the information of the gravitational slip parameter η in our likelihood analysis, this can be important for confronting the model with future high-precision observations of weak lensing.

IV. OBSERVATIONAL DATA

We would like to test for the model (2.15) with different observational data from CMB, BAO, SN Ia, the Hubble expansion rate, and RSD measurements. In this section, we will explain the data sets used in the likelihood analysis performed in Secs. V and VI.

A. CMB

The CMB power spectrum is affected by the presence of dark energy in at least two ways [2]. First, the positions of CMB acoustic peaks are shifted by the change of the angular diameter distance from the last scattering surface to today. Second, the variation of gravitational potentials induced by the presence of dark energy leads to the late-time integrated Sachs-Wolfe effect. The latter mostly affects the temperature anisotropies on large scales, at which the observational data are prone to uncertainties induced by the cosmic variance. Since the first effect is usually more important to constrain the property of dark energy, we will focus on the CMB distance measurements in the following.

The comoving distance to the CMB decoupling surface $r(z_*)$ (the redshift $z_* \simeq 1090$) and the comoving sound horizon at the CMB decoupling $r_{\rm s}(z_*)$ can be constrained from CMB measurements. In particular, the CMB shift parameters

$$\mathcal{R} = \sqrt{\Omega_{m0}}\, H_0 r(z_*)\,, \tag{4.1}$$

$$l_a = \frac{\pi r(z_*)}{r_{\rm s}(z_*)} \tag{4.2}$$

are the two key quantities for placing constraints on dark energy [57–59]. The shift parameter $\mathcal{R}$ is associated with the overall amplitude of CMB acoustic peaks, whereas l_a determines the average acoustic structure. We need to employ both $\mathcal{R}$ and l_a for extracting the necessary information to constrain dark energy models from the CMB power spectrum.

The comoving distance on the flat FLRW background is given by $r(z_*) = \int_0^{z_*} dz/H(z)$, where $z = a_0/a - 1$ is the redshift. Then, Eq. (4.1) reads

$$\mathcal{R} = \sqrt{\Omega_{m0}} \int_0^{z_*} \frac{dz}{E(z)}\,, \tag{4.3}$$

where $E(z)$ represents the Hubble ratio given by

$$E(z) \equiv \frac{H(z)}{H_0} = \sqrt{\frac{\Omega_{r0}}{\Omega_r}}(1+z)^2\,. \tag{4.4}$$

We can promote $\mathcal{R}$ to a function of z satisfying the condition $\mathcal{R}(0) = 0$. Defining the ratios $\bar{\Omega}_r = \Omega_r/\Omega_{r0}$ and $\bar{z} = z/z_*$, it follows that

$$\frac{d\mathcal{R}(\bar{z})}{d\bar{z}} = \frac{z_* \sqrt{\Omega_{m0}\bar{\Omega}_r}}{(1+z_*\bar{z})^2}\,, \tag{4.5}$$

which should be integrated from $\bar{z} = 0$ to $\bar{z} = 1$ with $\mathcal{R}(0) = 0$. In doing so, we need to know $\bar{\Omega}_r$ as a function of $\bar{z}$. For the model (2.15) with Eq. (2.16), the dark energy density parameter is known from Eq. (2.31), as

$$\Omega_{\rm DE} = (1 - \Omega_{m0} - \Omega_{r0})\, \bar{\Omega}_r^{1+s} (1+z_*\bar{z})^{-4(1+s)}\,. \tag{4.6}$$

On using Eq. (2.24), the radiation density parameter obeys

$$\frac{d\bar{\Omega}_r}{d\bar{z}} = \frac{z_* \bar{\Omega}_r [1 - \Omega_{r0}\bar{\Omega}_r + (3+4s)\,(1 - \Omega_{m0} - \Omega_{r0})\, \bar{\Omega}_r^{1+s} (1+z_*\bar{z})^{-4(1+s)}]}{(1+z_*\bar{z})[1 + s\,(1 - \Omega_{m0} - \Omega_{r0})\, \bar{\Omega}_r^{1+s} (1+z_*\bar{z})^{-4(1+s)}]}\,, \tag{4.7}$$

with $\bar{\Omega}_r(0) = 1$. We integrate Eqs. (4.5) and (4.7) to compute the value of $\mathcal{R}$ at $\bar{z} = 1$.

The dimensionless comoving distance $\bar{r}(z) = H_0 r(z)$, where $r(z) = \int_0^z dz'/H(z')$, obeys the differential equation

$$\frac{d\bar{r}(\bar{z})}{d\bar{z}} = \frac{z_* \sqrt{\bar{\Omega}_r}}{(1+z_*\bar{z})^2}\,, \tag{4.8}$$

where $\bar{r}(0) = 0$. The comoving sound horizon at the redshift z is defined by

$$r_{\rm s}(z) = \int_0^t \frac{c_{\rm s}\, dt}{a} = \frac{1}{H_0} \int_z^\infty dz' \frac{c_{\rm s}(z')}{E(z')}\,, \tag{4.9}$$

where we used the normalization $a_0 = 1$ in the second equality. The sound speed squared $c_{\rm s}$ of the coupled system of baryons (density ρ_b) and photons (density ρ_γ) is given by [60][1]

$$c_{\rm s} = \frac{1}{\sqrt{3[1 + R_b/(1+z)]}}\,, \tag{4.10}$$

[1] The quantity $c_{\rm s}$ is different from the sound speed c_S of the scalar degree of freedom ψ arising from the vector field. Since the density of the vector field is much smaller than those of the background fluids before the CMB decoupling epoch, the existence of the vector field does not affect $c_{\rm s}$.

where

$$R_b = \frac{3\rho_{b0}}{4\rho_{\gamma 0}} = 31500\Omega_{b0}\,h^2\left(\frac{2.7255}{2.7}\right)^{-4}. \tag{4.11}$$

Introducing the dimensionless quantity $\bar{r}_{\rm s} = H_0 r_{\rm s}$ and taking the z derivative of Eq. (4.9), we have $d\bar{r}_{\rm s}/dz = -c_{\rm s}(z)/E(z)$. Upon the change of variable, $\bar{a} = a/a_*$, it follows that $1+z = 1/a = 1/(a_*\bar{a}) = (1+z_*)/\bar{a}$. On using Eqs. (4.4) and (4.10), the dimensionless distance $\bar{r}_{\rm s}$ obeys the differential equation

$$\frac{d\bar{r}_{\rm s}}{d\bar{a}} = \frac{1}{1+z_*}\,\frac{\sqrt{\Omega_r(\bar{a})}}{\sqrt{3\Omega_{r0}[1+R_b\bar{a}/(1+z_*)]}}, \tag{4.12}$$

with $r_{\rm s}(\bar{a}=0)=0$.

The radiation density parameter is known from Eq. (2.24), such that

$$\frac{d\Omega_r}{d\bar{a}} = -\frac{\Omega_r[1-\Omega_r+(3+4s)\Omega_{\rm DE}]}{\bar{a}(1+s\,\Omega_{\rm DE})}. \tag{4.13}$$

At first glance the r.h.s. of Eq. (4.13) looks divergent in the limit $\bar{a}\to 0$, but this is not the case because the numerator also approaches 0. For numerical purposes, we will rewrite the r.h.s. of Eq. (4.13) in a more convenient form. In doing so, we introduce the following quantity

$$\Gamma \equiv \frac{\rho_r}{\rho_r+\rho_m} = \frac{\Omega_r}{\Omega_r+\Omega_m} = \frac{\Omega_r}{1-\Omega_{\rm DE}} = \frac{\Omega_{r0}(1+z_*)}{\Omega_{r0}(1+z_*)+\Omega_{m0}\bar{a}}. \tag{4.14}$$

Since $\Omega_r = \Gamma(1-\Omega_{\rm DE})$, the quantity $1-\Omega_r$ in Eq. (4.13) can be expressed as

$$1-\Omega_r = 1-\Gamma+\Gamma\Omega_{\rm DE} = \frac{\Omega_{m0}\bar{a}}{\Omega_{r0}(1+z_*)+\Omega_{m0}\bar{a}} + \frac{\Omega_{r0}(1+z_*)}{\Omega_{r0}(1+z_*)+\Omega_{m0}\bar{a}}\Omega_{\rm DE}, \tag{4.15}$$

where $\Omega_{\rm DE} = (1-\Omega_{m0}-\Omega_{r0})(1+z_*)^{-4(1+s)}(\Omega_r/\Omega_{r0})^{1+s}\bar{a}^{4(1+s)}$ from Eq. (2.31). Then, we can express Eq. (4.13) in the form

$$\begin{aligned}\frac{d\Omega_r}{d\bar{a}} &= -\frac{\Omega_r}{[1+s(1-\Omega_{m0}-\Omega_{r0})(\Omega_r/\Omega_{r0})^{1+s}(1+z_*)^{-4(1+s)}\bar{a}^{4(1+s)}]} \\ &\quad\times\left\{\frac{\Omega_{m0}}{\Omega_{r0}(1+z_*)+\Omega_{m0}\bar{a}} + \left[\frac{\Omega_{r0}(1+z_*)}{\Omega_{r0}(1+z_*)+\Omega_{m0}\bar{a}}+3+4s\right]\frac{(1-\Omega_{m0}-\Omega_{r0})\Omega_r^{1+s}\bar{a}^{3+4s}}{(1+z_*)^{4(1+s)}\Omega_{r0}^{1+s}}\right\},\end{aligned} \tag{4.16}$$

with $\Omega_r(\bar{a}\to 0)=1$. Provided that $3+4s>0$ we have $d\Omega_r/d\bar{a}\to -\Omega_{m0}/[\Omega_{r0}(1+z_*)]$ as $\bar{a}\to 0$, so the r.h.s. of Eq. (4.16) remains finite. Integrating Eqs. (4.12) and (4.16) with Eq. (4.8), the second CMB shift parameter $l_a = \pi\bar{r}(z_*)/\bar{r}_{\rm s}(z_*)$ can be computed accordingly.

The CMB shift parameters extracted from the Planck 2015 data have the mean values $\langle l_a\rangle = 301.77$ and $\langle\mathcal{R}\rangle = 1.7482$ with the deviations $\sigma(l_a)=0.090$ and $\sigma(\mathcal{R})=0.0048$, respectively [61]. We fix the baryon density parameter as $\Omega_b h^2 = 0.02226$, where h is the normalized Hubble constant ($H_0 = 100\,h$ km s^{-1} Mpc^{-1}). The components of the normalized covariance matrix $\boldsymbol{C}$ are given by $C_{11}=C_{22}=1$ and $C_{12}=C_{21}=0.3996$. Then, the χ^2 statistics associated with the CMB shift parameters is given by[2]

$$\chi^2_{\rm CMB} = (l_a-301.77)^2\times 146.916 + (\mathcal{R}-1.7482)^2\times 51650.31 + 2(\mathcal{R}-1.7482)(l_a-301.77)\times(-1100.77). \tag{4.17}$$

The dependence on the parameters Ω_{m0}, h and s are encoded in $\mathcal{R}$ and l_a. For the test parameters $\Omega_{m0}=0.3$, $h=0.6774$, and $s=0.1$, we find that $\chi^2_{\rm CMB}=1519.87$.

---

[2] The Planck 2015 team [62] provided the values $l_a = 301.76\pm 0.14$ and $\mathcal{R}=1.7488\pm 0.0074$ with the covariance matrix components $C_{11}=C_{22}=1$ and $C_{12}=C_{21}=0.54$. We confirm that the corresponding $\chi^2_{\rm CMB}$ analysis gives very similar likelihood results as those derived from Eq. (4.17).

B. BAO

We also use the BAO data to constrain our model further. The BAO represent periodic fluctuations of the density of baryonic matter as a result of the counteracting forces of pressure and gravity. The photons release a pressure after the decoupling, which on the other hand creates a shell of baryonic matter at the sound horizon. From the BAO measurements we can deduce the distance-redshift relation at the observed redshifts. One of the important quantities is the sound horizon $r_{\rm s}(z_d)$, where z_d is the redshift at which baryons are released from photons. There is a fitting formula for the drag redshift z_d, as [63]

$$z_d = \frac{1291(\Omega_{m0}h^2)^{0.251}}{1+0.659(\Omega_{m0}h^2)^{0.828}}\left[1+b_1(\Omega_b h^2)^{b_2}\right], \tag{4.18}$$

where the parameters b_1 and b_2 are

$$b_1 = 0.313(\Omega_{m0}h^2)^{-0.419}\left[1+0.607(\Omega_{m0}h^2)^{0.674}\right], \tag{4.19}$$

$$b_2 = 0.238(\Omega_{m0}h^2)^{0.223}. \tag{4.20}$$

The sound horizon $r_{\rm s}(z)$ is given by Eq. (4.9) with the sound speed (4.10). We perform a change of the variable $\tilde{a} = a/a_d$ with $1+z = a_0/(a_d\tilde{a}) = (1+z_d)/\tilde{a}$. This helps us to make use of some of the results in the CMB distance measurements. Since $\tilde{a}/\bar{a} = (1+z_d)/(1+z_*)$, it follows that $\bar{a}(a=a_d) = (1+z_*)/(1+z_d)$. With this change of variables, we can now integrate Eq. (4.16) from $\bar{a}=0$ to $\bar{a} = (1+z_*)/(1+z_d)$. For the test parameters $\Omega_{m0}=0.3$, $h=0.6774$ and $s=0.1$, we obtain the value $\bar{r}_{\rm s}(z_d) = 0.03437$. We also need to compute the diameter distance

$$D_A(z) = \frac{1}{H_0(1+z)}\int_0^z \frac{dz'}{E(z')}. \tag{4.21}$$

The dimensionless quantity $\bar{D}_A = H_0 D_A$ is known by integrating the following differential equations:

$$\frac{d\bar{D}_A}{dz} = -\frac{\bar{D}_A}{1+z} + \frac{\sqrt{\bar{\Omega}_r}}{(1+z)^3}, \tag{4.22}$$

$$\frac{d\bar{\Omega}_r}{dz} = \frac{\bar{\Omega}_r[1-\Omega_{r0}\bar{\Omega}_r + (3+4s)(1-\Omega_{m0}-\Omega_{r0})\bar{\Omega}_r^{1+s}(1+z)^{-4(1+s)}]}{(1+z)[1+s(1-\Omega_{m0}-\Omega_{r0})\bar{\Omega}_r^{1+s}(1+z)^{-4(1+s)}]}, \tag{4.23}$$

with $\bar{D}_A(z=0)=0$. With the diameter distance, we are now at a place to compute the dilation scale [64]

$$D_V(z) = \left[(1+z)^2 D_A^2(z)\, z\, H^{-1}(z)\right]^{1/3} = \left[D_A^2(z)\, z\, H_0^{-1}\sqrt{\bar{\Omega}_r(z)}\right]^{1/3}. \tag{4.24}$$

The important observable is the ratio between the sound horizon at the drag redshift and the dilation scale

$$\frac{r_{\rm s}(z_d)}{D_V(z)} = \frac{\bar{r}_{\rm s}(z_d)}{(\bar{D}_A^2(z)\, z\sqrt{\bar{\Omega}_r})^{1/3}}, \tag{4.25}$$

which is dimensionless and does not depend on H_0.

We use the BAO data from the 6dFGS [65], SDSS-MGS [66], BOSS [67], BOSS CMASS [68], and Wiggle Z [69] surveys. Then, the χ^2 statistics in BAO measurements is given by

$$\begin{aligned}
\chi^2_{\rm BAO} &= \frac{1}{0.015^2}\left[\frac{r_{\rm s}(z_d)}{D_V(z=0.106)} - 0.336\right]^2 + \frac{1}{\left(\frac{25}{148.69}\right)^2}\left[\frac{D_V(z=0.15)}{r_{\rm s}(z_d)} - \frac{664}{148.69}\right]^2 \\
&+ \frac{1}{\left(\frac{25}{149.28}\right)^2}\left[\frac{D_V(z=0.32)}{r_{\rm s}(z_d)} - \frac{1264}{149.28}\right]^2 + \frac{1}{\left(\frac{16}{147.78}\right)^2}\left[\frac{D_V(z=0.38)}{r_{\rm s}(z_d)} - \frac{1477}{147.78}\right]^2 \\
&+ \frac{1}{0.0071^2}\left[\frac{r_{\rm s}(z_d)}{D_V(z=0.44)} - 0.0916\right]^2 + \frac{1}{\left(\frac{19}{147.78}\right)^2}\left[\frac{D_V(z=0.51)}{r_{\rm s}(z_d)} - \frac{1877}{147.78}\right]^2 \\
&+ \frac{1}{\left(\frac{20}{149.28}\right)^2}\left[\frac{D_V(z=0.57)}{r_{\rm s}(z_d)} - \frac{2056}{149.28}\right]^2 + \frac{1}{0.0034^2}\left[\frac{r_{\rm s}(z_d)}{D_V(z=0.6)} - 0.0726\right]^2 \\
&+ \frac{1}{\left(\frac{22}{147.78}\right)^2}\left[\frac{D_V(z=0.61)}{r_{\rm s}(z_d)} - \frac{2140}{147.78}\right]^2 + \frac{1}{0.0032^2}\left[\frac{r_{\rm s}(z_d)}{D_V(z=0.73)} - 0.0592\right]^2.
\end{aligned} \tag{4.26}$$

For the test parameters mentioned above Eq. (4.21), we find that $\chi^2_{\rm BAO} = 10.443$.

C. SN Ia

The SN Ia can be used as standard candles with known brightness to refer to physical distances. This is based on the fact that the logarithm of an astronomical object's luminosity seen from a distance of 10 parsecs gives its absolute magnitude M, which on the other hand enables us to refer to its brightness. For SN Ia the absolute magnitude at the peak of brightness is nearly constant ($M \simeq -19$). If a supernova at a given redshift z is observed with the apparent magnitude m, then the difference between m and M is related to a luminosity distance $d_L(z)$, as

$$\mu(z) \equiv m(z) - M = 5 \log \bar{d}_L(z) - 5 \log h + \mu_0 \,, \tag{4.27}$$

where $\mu_0 = 42.38$, and

$$\bar{d}_L(z) \equiv H_0 d_L(z) = (1+z) \int_0^z \frac{dz'}{E(z')} \,. \tag{4.28}$$

The Hubble expansion rate $H(z)$ is known by measuring $m(z)$ for many different redshifts ($z \lesssim 3$), which allows one to constrain dark energy models [70, 71].

With the distance modulus of our model at hand, we can directly compare it with the supernova data and compute the χ^2 estimator

$$\chi^2_{\rm SNIa} = \sum_{i=1}^{N} \frac{[\mu_{\rm obs}(z_i) - \mu_{\rm th}(z_i)]^2}{\sigma_i^2} \,, \tag{4.29}$$

where N is the number of the SN Ia data set, $\mu_{\rm obs}(z_i)$ and $\mu_{\rm th}(z_i)$ are the observed and theoretical values of the distance modulus $\mu(z_i)$, respectively, and σ_i are the errors on the data. Since the SN Ia data are in the low-redshift regime, we can neglect the contribution of radiation and set $\Omega_r = 0$. Furthermore, due to the degeneracy between the absolute magnitude and h, we will marginalize over h. For the likelihood analysis, we use the Union 2.1 data sets [72].

D. Local measurements of the Hubble expansion rate

The recent observations of Cepheids in galaxies of SN Ia placed the bound on the local value of normalized Hubble constant H_0, as [73]

$$h = 0.7324 \pm 0.0174 \,. \tag{4.30}$$

With the knowledge of the comoving sound horizon it is possible to extract the information of the Hubble expansion rate from BAO measurements, as

$$H(z)\, r_s(z_d) = E(z)\, \bar{r}_s(z_d) = \frac{(1+z)^2}{\sqrt{\bar{\Omega}_r}} \bar{r}_s(z_d) \,. \tag{4.31}$$

For this purpose we use the recent BOSS data [67] in addition to the bound (4.30). Thus, we define the χ^2 statistics associated with the local measurements of H as follows

$$\begin{aligned} \chi^2_H \;=\; & \frac{(h-0.7324)^2}{0.0174^2} + \frac{\left[H(z=0.38)\, r_s(z_d) - 81.5 \times 147.78/299792.458\right]^2}{(2.6 \times 147.78/299792.458)^2} \\ & + \frac{\left[H(z=0.51)\, r_s(z_d) - 90.5 \times 147.78/299792.458\right]^2}{(2.6 \times 147.78/299792.458)^2} \\ & + \frac{\left[H(z=0.61)\, r_s(z_d) - 97.3 \times 147.78/299792.458\right]^2}{(2.9 \times 147.78/299792.458)^2} \,. \end{aligned} \tag{4.32}$$

For the test parameters $\Omega_{m0} = 0.3$, $h = 0.6774$, and $s = 0.1$, we obtain $\chi^2_H = 30.43$.

E. RSD

For the perturbations relevant to the RSD measurements (sub-horizon modes with $k \gg aH$) it was shown in Ref. [42] that the quasi-static approximation is sufficiently accurate to describe the evolution of the matter density contrast δ, so we resort to Eq. (3.31) without taking into account the radiation ($\Omega_r = 0$). In terms of the derivative with respect to $\mathcal{N} = \ln a$, we can rewrite Eq. (3.31) in the form

$$\delta'' + \frac{1-3w_{\rm eff}}{2}\delta' - \frac{4\pi G_{\rm eff}\rho_m}{H^2}\delta = 0\,, \tag{4.33}$$

where $w_{\rm eff} = -1 - 2\dot{H}/(3H^2)$ is the effective equation of state whose explicit form in our model is given by Eq. (2.26). On using the matter density parameter $\Omega_m = 8\pi G\rho_m/(3H^2)$, where $G = 1/(8\pi M_{\rm pl}^2)$ is the bare gravitational constant, Eq. (4.33) reduces to

$$\delta'' + \frac{1+(3+4s)\Omega_{\rm DE}}{2(1+s\Omega_{\rm DE})}\delta' - \frac{3}{2}\frac{G_{\rm eff}}{G}(1-\Omega_{\rm DE})\delta = 0\,. \tag{4.34}$$

For the integration of this differential equation, we use the effective gravitational coupling given by Eq. (3.32).

The ΛCDM model corresponds to $s = 0$ and $G_{\rm eff} = G$ in Eq. (4.34), in which case there is the growing-mode solution $\delta \propto a$ during the matter dominance ($\Omega_{\rm DE} \simeq 0$). In our model $\Omega_{\rm DE} \simeq 0$ and $G_{\rm eff} \simeq G$ in the early matter era, so the evolution of δ at high redshifts ($z \gg 1$) is very similar to that in the ΛCDM model. Hence we choose the initial conditions satisfying $\delta = \delta'$ in the deep matter era. The difference from the ΛCDM model arises at low redshifts where $\Omega_{\rm DE}$ and $G_{\rm eff}$ deviate from 0 and G, respectively.

We define σ_8 as the amplitude of over-density at the comoving $8\,h^{-1}$ Mpc scale. To compute the χ^2 estimator of RSD measurements, we introduce the following quantity

$$y(z) \equiv f(z)\sigma_8(z)\,, \qquad f(z) \equiv \frac{\delta'}{\delta}\,. \tag{4.35}$$

Since the behavior of perturbations in our model is very close to that in the ΛCDM model at high redshifts, the two models should have similar initial conditions of δ. This implies that $\sigma_8^{\rm Proca}(z_i) \approx \sigma_8^{\Lambda{\rm CDM}}(z_i)$ at an initial redshift $z = z_i \gg 1$. Since we assume that the radiation is negligible, we choose such an initial redshift to be in the deep matter era, that is, at $N_i = -6$ (around $z_i \simeq 400$).

For the $f\sigma_8$ data extracted from RSD measurements, we use those listed in Table I of Ref. [74]. This includes the recent data of FastSound at the redshift $z = 1.36$ [75]. We define the χ^2 estimator, as

$$\chi^2_{\rm RSD} = \sum_{i=1}^{N} \frac{[y_{\rm obs}(z_i) - y_{\rm th}(z_i)]^2}{\sigma_i^2}\,, \tag{4.36}$$

where N is the number of the RSD data, $y_{\rm obs}(z_i)$ and $y_{\rm th}(z_i)$ are the observed and theoretical values of $y(z_i)$ at redshift z_i respectively, and σ_i's are the errors on the data.

Among other measurements discussed in this section, the RSD data are only those strictly connected with the growth of perturbations. Since the effective gravitational coupling (3.32) depends on many model parameters like q_V and c_S^2, there should be some level of degeneracy of model parameters compared to the analysis based on the background expansion history. Reflecting this situation, we will focus on the case $\beta_5 = 0$ for the likelihood analysis including the RSD data.

V. BACKGROUND CONSTRAINTS

As a first analysis of the theory, we study how the background cosmic expansion history can fit the observational data sets of CMB, BAO, SN Ia, and the Hubble expansion rate. In this section we do not take into account the RSD data, as they directly deal with the growth of matter perturbations. Then, we focus on the likelihood analysis for the following parameters:

$$\Omega_{m0}, \quad h, \quad s\,. \tag{5.1}$$

The analysis of the background alone is simpler than the one including the perturbations, as the space of parameters reduces to a three-dimensional one. It should be noticed that, compared to the ΛCDM model, our model has only

one additional background parameter, s. Furthermore, the ΛCDM model corresponds to $s = 0$ at the background level, so the direct comparison between the two models is straightforward.

For the Monte-Carlo-Markov-Chain (MCMC) sampling, we need to put some priors on the allowed parameter space of the three parameters. We will choose sensible priors for the parameters (5.1) as follows:

- For the density parameter of non-relativistic matter, $0.1 \leq \Omega_{m0} \leq 0.5$.
- For the normalized Hubble constant, $0.6 \leq h \leq 0.8$.
- For the deviation parameter s from the ΛCDM model, $-0.3 \leq s \leq 0.8$.

Since the analysis including perturbations is not performed in this section, we do not put priors on the quantities associated with perturbations (e.g., $q_V > 0$, $c_S^2 > 0$ etc). As we will see in Sec. VI, some of the results can change by taking into account perturbations and the allowed parameter space may be reduced. Nonetheless, it is worthy of investigating first how our model can fit the data at the background level compared to the ΛCDM model. We perform the MCMC sampling over the allowed three-dimensional parameter space and compute

$$\chi^2_{\rm back} = \chi^2_{\rm CMB} + \chi^2_{\rm BAO} + \chi^2_{\rm SNIa} + \chi^2_H \,. \tag{5.2}$$

The best fit corresponds to the case in which $\chi^2_{\rm back}$ is minimized.

In Fig. 1 we plot one-dimensional probability distributions of the parameters (5.1) and two-dimensional observational contours for the combination of these three parameters. The one-dimensional probability distributions show that the minimum value of $\chi^2_{\rm back}$ does exist for the following (approximated) values:

$$\Omega_{m0} = 0.3027\,, \qquad h = 0.6981\,, \qquad s = 0.254\,, \tag{5.3}$$

for which

$$\chi^2_{\rm back,min} \approx 590.4\,. \tag{5.4}$$

The existence of a minimum around $s = 0.25$ shows that the model with $s > 0$ is favored over the ΛCDM model at the background level. The 2σ constraints on the three parameters are given by

$$\Omega_{m0} = 0.3027^{+0.0060}_{-0.0057}\,, \tag{5.5}$$

$$h = 0.6981^{+0.0059}_{-0.0057}\,, \tag{5.6}$$

$$s = 0.254^{+0.118}_{-0.097}\,. \tag{5.7}$$

This means that the ΛCDM model is disfavored over the model with $s > 0$ even at the 2σ level. We note that the extended scalar Galileon model [76] has a tracker solution whose background evolution is the same as that in the model under consideration. In Ref. [77] two of the present authors performed the likelihood analysis by using the data of the CMB (WMAP7), BAO, SN Ia, and derived the bound $s = 0.034^{+0.327}_{-0.034}$ (95 % CL). With the new data of the CMB (Planck), BAO, SN Ia, and the Hubble expansion rate, the constraint on s is shifted toward larger values.

In the ΛCDM model, the best-fit values of Ω_{m0} and h constrained by the Planck CMB data are around $\Omega_{m0} \approx 0.31$ and $h \approx 0.68$, respectively [78]. These best-fit values are in tension with their low-redshift measurements, which generally favor lower Ω_{m0} and higher h, see, e.g., Eq. (4.30). The model with $s > 0$ can reduce such a tension with the shift toward smaller Ω_{m0} and larger h. We can confirm this property in the probability distributions of Ω_{m0} and h in Fig. 1.

VI. OBSERVATIONAL CONSTRAINTS INCLUDING THE RSD DATA

If we take into account the evolution of matter perturbations, the likelihood results can be subject to change in two different ways: 1) the stability conditions of perturbations, which need to hold at all times, generally reduce the allowed parameter space; and 2) the RSD contribution can shift observational bounds of model parameters. We set the following additional priors to those used in Sec. V:

- The no-ghost conditions for scalar, vector, and tensor perturbations to apply at all times, i.e., $q_T > 0, q_V > 0, Q_S > 0$.
- The stability conditions associated with the propagation speeds of scalar, vector, and tensor perturbations, i.e., $c_T^2 > 0, c_V^2 > 0, c_S^2 > 0$. We also put the priors that c_T^2, c_V^2, c_S^2 are initially smaller than 10^3 to avoid the divergences of these quantities in the asymptotic past.

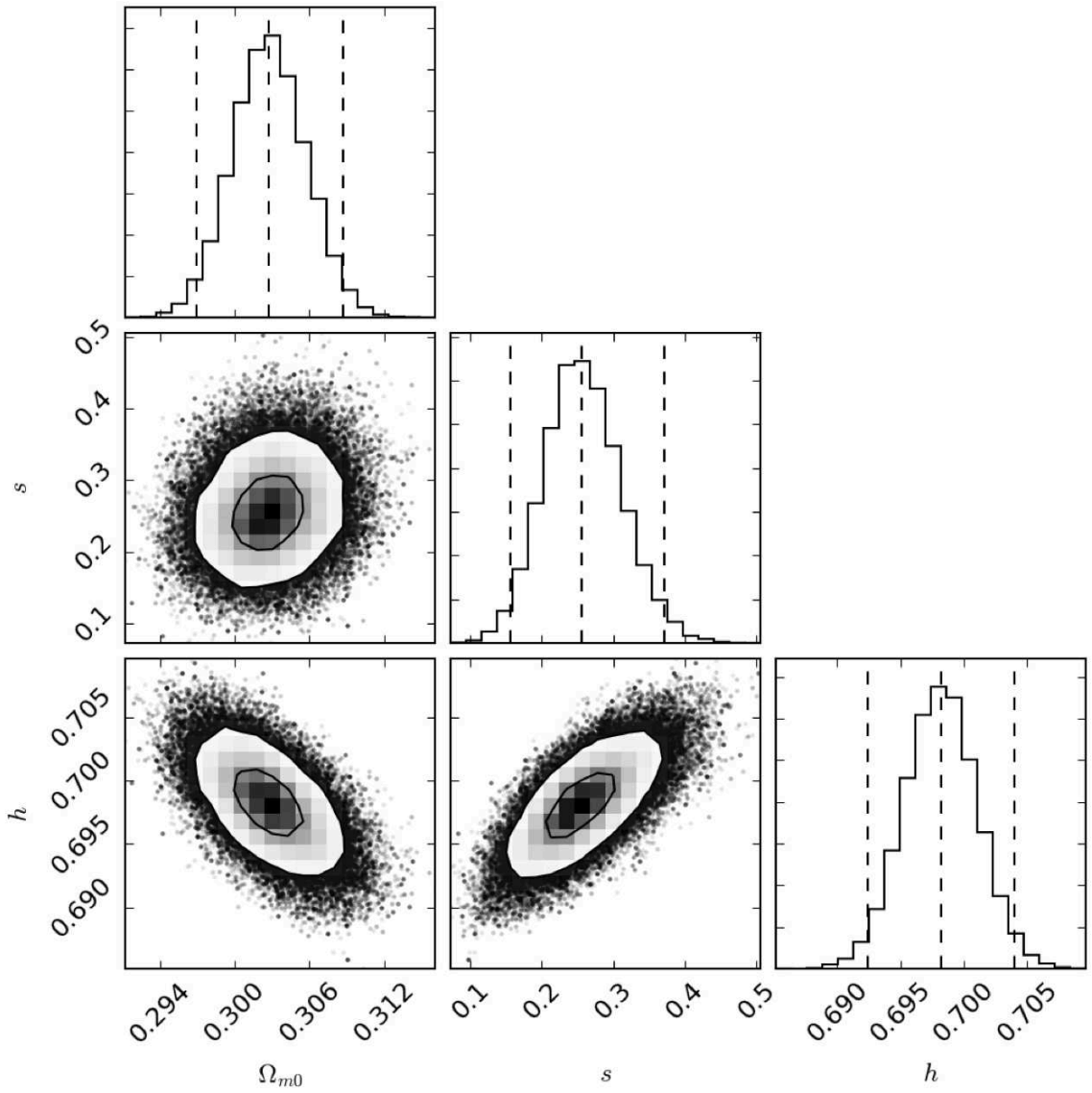


FIG. 1: Observational bounds on the three parameters Ω_{m0}, s, h constrained by the data of the CMB, BAO, SN Ia, and the Hubble expansion rate. The RSD data are not taken into account in the analysis. Since the analysis is based on the background cosmic expansion history, we do not consider the conditions associated with ghosts and stabilities of perturbations. From top to bottom, the right panels in each column are one-dimensional probability distributions of the parameters Ω_{m0}, s, h, respectively. The vertical dashed lines correspond to the best fit (central) and the 2σ confidence limits (outside). The other panels are the two-dimensional likelihood contours in the (s, Ω_{m0}), (h, Ω_{m0}), and (h, s) planes with 1σ (inside) and 2σ (outside) boundaries. The ΛCDM model, which corresponds to $s = 0$, is disfavored over the model with $s > 0$ from the background analysis.

- The condition $c_T^2 > 1$ to be valid *today*. This is for evading the Cherenkov radiation bound $1 - c_T < 2 \times 10^{-15}$ today [79, 80].
- $0 < p \leq 25$ for keeping the parameter p positive and of order unity.
- $-10^3 \leq \beta \leq -10^{-9}$, $10^{-13} \leq \lambda \leq 15$. The reason for the choices of negative β and positive λ were explained in Sec. II B. We choose flat distributions for the natural logarithms of these variables.

- $-4 \leq \ln(q_V) \leq 15$. We choose the values of q_V to be not very close to 0 to avoid the strong coupling problem.

For simplicity we set the parameter β_5 to zero, as keeping it non-zero in the analysis does not change the final results significantly. The likelihood results seem to be flat in this direction, such that the observational data do not notably constrain this parameter.

We perform a MCMC analysis and compute

$$\chi^2 = \chi^2_{\rm CMB} + \chi^2_{\rm BAO} + \chi^2_{\rm SNIa} + \chi^2_H + \chi^2_{\rm RSD}\,, \tag{6.1}$$

in order to quantify how the RSD data affect the available parameter space constrained at the background level. We verify that the role of no-ghost and stability conditions is important, because some of the parameter space preferred by the background analysis (performed in Sec. V) does not possess a stable cosmological evolution. For example, the best fit obtained by the background analysis does not in general satisfy no-ghost conditions of perturbations. Furthermore we find that the RSD data affect constraints on some parameters like p, but they only give mild bounds on other parameters such as β, λ, q_V. Nonetheless, the RSD data also contribute to shifting/reducing the parameter space for the background parameters Ω_{m0}, h, s, because the matter perturbation equation depends on those parameters.

The MCMC likelihood analysis shows that there is a quite large degeneracy in terms of the minimum χ^2, i.e., several different parameters associated with perturbations can lead to similar values of χ^2. In other words, the model does not seem to have one unique global minimum of χ^2, but there are several of those minima for different sets of parameters. We can pick up one example of such a low value of χ^2. For instance, we obtain the minimum value

$$\chi^2_{\rm min} = 625.6\,, \tag{6.2}$$

for the following (approximated) values:

$$\begin{aligned} &\Omega_{m0} = 0.299\,, \qquad h = 0.6962\,, \qquad s = 0.16\,, \\ &p = 2.69\,, \qquad \ln(-\beta) = 0.33\,, \qquad \ln q_V = -1.731\,, \qquad \ln\lambda = -16.9\,. \end{aligned} \tag{6.3}$$

The corresponding 2σ bounds on these parameters are given, respectively, by

$$\Omega_{m0} = 0.299^{+0.006}_{-0.006}\,, \tag{6.4}$$

$$h = 0.696^{+0.006}_{-0.005}\,, \tag{6.5}$$

$$s = 0.16^{+0.08}_{-0.08}\,, \tag{6.6}$$

$$p = 2.69^{+19.91}_{-0.73}\,, \tag{6.7}$$

$$\beta = -1.39^{+0.75}_{-492.28}\,, \tag{6.8}$$

$$\bar{q}_V \leq q_V < 164\,, \tag{6.9}$$

$$\bar{\lambda} \leq \lambda < 0.015\,, \tag{6.10}$$

where $\bar{q}_V$ and $\bar{\lambda}$ are the lower limits from the assumed prior/numerical precision.

The probability distributions and the likelihood contours for the background parameters Ω_{m0}, s, h and the full parameters $\Omega_{m0}, s, h, p, \beta, q_V, \lambda$ are plotted in Figs. 2 and 3, respectively. The RSD data together with the stability conditions influence the parameter space in several ways. We summarize the main results in the following.

- Inclusion of the RSD data tends to reduce the best-fit value of s (compared to $s \simeq 0.26$ constrained from the background), but still a positive value of s around 0.16 is favored, see Fig. 2. This implies that the RSD data generally prefer the model with lower s. Indeed, the RSD data alone can be consistent with the case $s = 0$. This is mostly attributed to the fact that the models with a larger s tend to give rise to a larger effective gravitational coupling with $G_{\rm eff} > G$. There is a tendency that the current RSD measurements favor the cosmic growth rate smaller than that predicted by GR [62]. In generalized Proca theories it is possible to realize $G_{\rm eff} < G$, but this occurs at the expense of choosing the value of q_V close to 0 [42]. To avoid the strong coupling problem of vector perturbations we set the prior $q_V \lesssim 10^{-2}$, in which case $G_{\rm eff}$ cannot be significantly smaller than G. Since the effect of weak gravity arising from small q_V is limited, the modification of $G_{\rm eff}$ induced by the change of s tends to be more important. In Fig. 3 we observe that the parameter q_V is loosely constrained.

- The data other than RSD favor a non-zero positive value of s. Therefore, combining all these different contributions, we obtain the bound (6.6), which is smaller than $s = 0.25$. On performing a MCMC sampling for the ΛCDM model with the two parameters Ω_{m0} and h, we find that the best-fit case corresponds to $\chi^2_{\Lambda\rm CDM} = 642.7$ with $\Omega_{m0} = 0.298$ and $h = 0.688$. Since this value of χ^2 is larger than (6.2), the model with $s \approx 0.16$ can fit the joint observational constraints of the CMB, BAO, SN Ia, the Hubble expansion rate, and RSD better than the ΛCDM model.

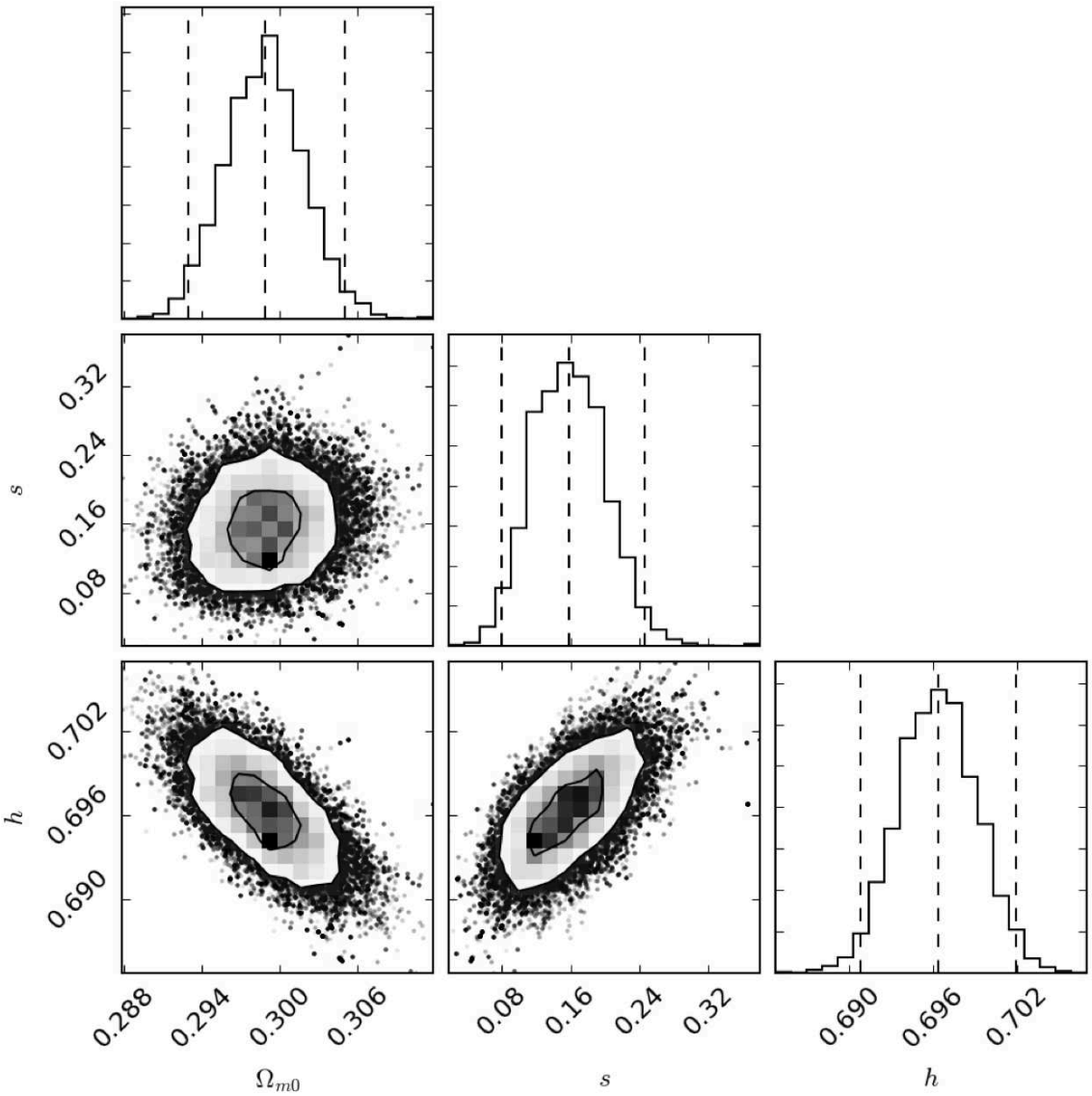


FIG. 2: Observational bounds on the three parameters Ω_{m0}, s, h derived by adding the RSD data to the data of the CMB, BAO, SN Ia, and the Hubble expansion rate. The no-ghost and stability conditions are also taken into account. The meanings of one-dimensional probability distributions and two-dimensional likelihood contours are the same as those explained in the caption of Fig. 1. The ΛCDM model is still disfavored over the model with $s > 0$.

- Comparing the bounds (6.4) and (6.5) with Eqs. (5.5) and (5.6), the constraints on Ω_{m0} and h derived by adding the RSD data to the data associated with the background expansion history are not subject to significant modifications relative to those obtained without the RSD data.

- Since only the RSD data are affected by the four parameters p, β, q_V, λ associated with perturbations, we find that the constraints on them are mild and that some degeneracy of χ^2 exists among different model parameters. We expect that this degeneracy may be reduced by including other independent observational data relevant to perturbations.

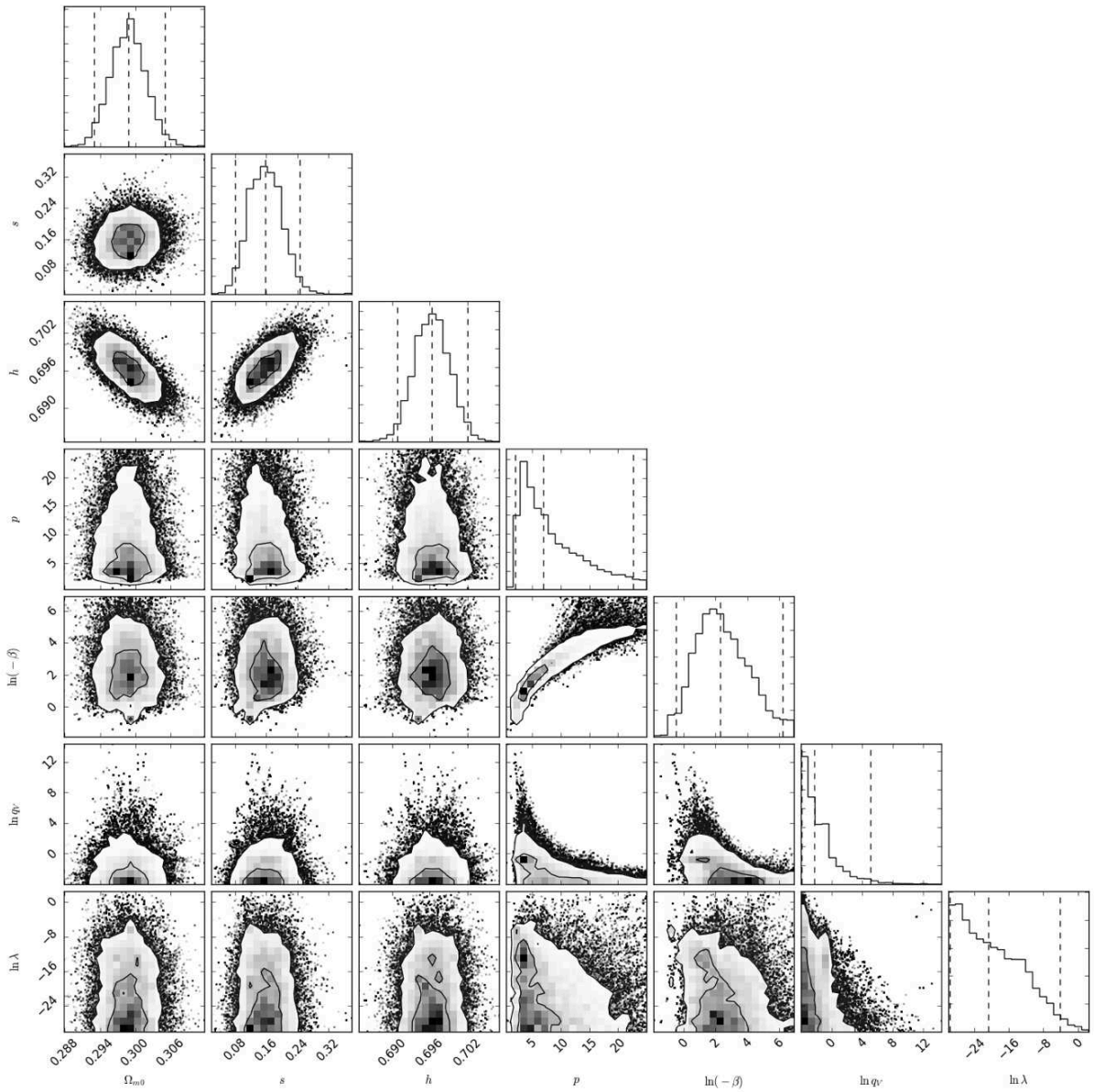


FIG. 3: Observational constraints on the seven model parameters $\Omega_{m0}, s, h, p, \beta, q_V, \lambda$ derived by the joint data analysis of the CMB, BAO, SN Ia, the Hubble expansion rate, and RSD data, with no-ghost and stability conditions taken into account. The meanings of one-dimensional probability distributions and two-dimensional likelihood contours are the same as those explained in the caption of Fig. 1. The three parameters Ω_{m0}, s, h associated with the background are tightly constrained, but the bounds on the four parameters p, β, q_V, λ are quite weak.

VII. CONCLUSIONS

The recently proposed generalized Proca interactions constitute promising alternative theories of gravity on large scales. These derivative vector-tensor interactions are constructed in such a way that the resulting theories contain only five propagating degrees of freedom, three of them originating from the massive vector field [35, 37, 38]. They establish a consistent framework for the late-time cosmic acceleration. On the FLRW background, the temporal component of the vector field gives rise to interesting de Sitter solutions relevant to dark energy. Even if the temporal component is not dynamical, its auxiliary role results in promising de Sitter attractors as it was shown in Ref. [41].

In this work, we have placed observational constraints on a class of dark energy models in the framework of

generalized Proca theories. We have first summarized the key findings of the background evolution and stability analysis of perturbations performed in Refs. [41, 42]. The background dynamics is rather simple and dictated by the three parameters Ω_{m0}, h, s, where s represents the deviation from the ΛCDM model. For the evolution of matter perturbations, we have used the equation derived under the quasi-static approximation on sub-horizon scales, whose validity was explicitly checked in Ref. [42]. We have also taken into account conditions for avoiding ghosts and Laplacian instabilities of tensor, vector, and scalar perturbations. The perturbations carry four additional parameters p, β, q_V, λ than those associated with the background.

At the background level, we have exploited the data sets of CMB distance priors, BAO, SN Ia (Union 2.1), and local measurements of the Hubble expansion rate. We have found that the MCMC analysis constrains the parameter s to be $s = 0.254^{+0.118}_{-0.097}$ (95 % CL) from the background cosmic expansion history, so the model with $s > 0$ can have a good fit to the data compared to the ΛCDM model. This is attributed to the fact that existence of the additional parameter s can reduce the tensions of the parameters Ω_{m0} and h between early-time and late-time data sets.

Including the RSD data as well as no-ghost and stability conditions of perturbations, the bound on the parameter s is shifted to $s = 0.16^{+0.08}_{-0.08}$ (95 % CL). This shift is mostly related to the fact that the RSD data tend to favor lower values of s for realizing $G_{\rm eff}$ close to G. Existence of the intrinsic vector mode can lead to a $G_{\rm eff}$ smaller than G for q_V close to 0, but this effect is limited by the fact that the vector perturbation has a strong coupling problem for such small values of q_V. Since the data other than RSD prefer positive values of s away from 0, the joint data analysis including both the background and the RSD data still favor the model with $s > 0$ over the ΛCDM model. We have also found that, expect for the background quantities Ω_{m0}, h, s, the observational bounds on other parameters are not stringent.

As we have seen in this work, the derivative interactions in generalized Proca theories facilitate the background evolutions quite generically, which give rise to the dynamics for alleviating the tension between early-time and late-time data sets. It is still possible that the tension present in the ΛCDM model may be related to some systematic errors in one (or more) data sets. Nonetheless, we find it interesting at least to have shown that the cosmological background fitting the data well can naturally follow from generalized Proca theories.

We note that beyond-generalized Proca theories recently proposed in Ref. [39] share the same background evolution as the model (2.15). Nevertheless, the presence of additional terms yields distinctive features at the level of perturbations. For instance, it is possible to weaken the gravitational coupling with non-relativistic matter further, e.g., $G_{\rm eff} \approx 0.8G$ today [81]. The smaller effective gravitational coupling, which may fit the RSD data better than the model studied in this paper, arise from beyond-generalized Proca interactions rather than from intrinsic vector modes with q_V close to 0. It will be of interest to place observational constraints on such models as well by adding other data associated with perturbations, e.g., the integrated Sachs-Wolfe effect of CMB and weak lensing. We hope that future high-precision observations will allow us to distinguish the models in the framework of (beyond-)generalized Proca theories from the ΛCDM model further.

Acknowledgments

ADF is supported by the JSPS KAKENHI Grant Numbers 16K05348 and 16H01099. LH acknowledges financial support from Dr. Max Rössler, the Walter Haefner Foundation and the ETH Zurich Foundation. ST is supported by the Grant-in-Aid for Scientific Research Fund of the JSPS No. 16K05359 and a MEXT KAKENHI Grant-in-Aid for Scientific Research on Innovative Areas "Cosmic Acceleration" (No. 15H05890).

[1] S. Weinberg, Rev. Mod. Phys. **61**, 1 (1989).
[2] E. J. Copeland, M. Sami and S. Tsujikawa, Int. J. Mod. Phys. D **15**, 1753 (2006) [hep-th/0603057].
[3] T. P. Sotiriou and V. Faraoni, Rev. Mod. Phys. **82**, 451 (2010) [arXiv:0805.1726 [gr-qc]].
[4] A. De Felice and S. Tsujikawa, Living Rev. Rel. **13**, 3 (2010) [arXiv:1002.4928 [gr-qc]].
[5] T. Clifton, P. G. Ferreira, A. Padilla and C. Skordis, Phys. Rept. **513**, 1 (2012) [arXiv:1106.2476 [astro-ph.CO]].
[6] L. Amendola *et al.* [Euclid Theory Working Group], Living Rev. Rel. **16**, 6 (2013) [arXiv:1206.1225 [astro-ph.CO]].
[7] A. Joyce, B. Jain, J. Khoury and M. Trodden, Phys. Rept. **568**, 1 (2015) [arXiv:1407.0059 [astro-ph.CO]].
[8] P. Bull *et al.*, Phys. Dark Univ. **12**, 56 (2016) [arXiv:1512.05356 [astro-ph.CO]].
[9] L. Amendola *et al.*, arXiv:1606.00180 [astro-ph.CO].
[10] C. M. Will, Living Rev. Rel. **9**, 3 (2006) [gr-qc/0510072].
[11] A. I. Vainshtein, Phys. Lett. **39B**, 393 (1972).
[12] C. Deffayet, G. R. Dvali and G. Gabadadze, Phys. Rev. D **65**, 044023 (2002) [astro-ph/0105068].
[13] E. Babichev, C. Deffayet and R. Ziour, Phys. Rev. Lett. **103**, 201102 (2009) [arXiv:0907.4103 [gr-qc]].

[14] C. Burrage and D. Seery, JCAP **1008**, 011 (2010) [arXiv:1005.1927 [astro-ph.CO]].
[15] A. De Felice, R. Kase and S. Tsujikawa, Phys. Rev. D **85**, 044059 (2012) [arXiv:1111.5090 [gr-qc]].
[16] R. Kimura, T. Kobayashi and K. Yamamoto, Phys. Rev. D **85**, 024023 (2012) [arXiv:1111.6749 [astro-ph.CO]].
[17] R. Kase and S. Tsujikawa, JCAP **1308**, 054 (2013) [arXiv:1306.6401 [gr-qc]].
[18] A. Nicolis, R. Rattazzi and E. Trincherini, Phys. Rev. D **79**, 064036 (2009) [arXiv:0811.2197 [hep-th]].
[19] C. Deffayet, G. Esposito-Farese and A. Vikman, Phys. Rev. D **79**, 084003 (2009) [arXiv:0901.1314 [hep-th]].
[20] C. Deffayet, S. Deser and G. Esposito-Farese, Phys. Rev. D **80**, 064015 (2009) [arXiv:0906.1967 [gr-qc]].
[21] C. Burrage, C. de Rham and L. Heisenberg, JCAP **1105**, 025 (2011) [arXiv:1104.0155 [hep-th]].
[22] G. W. Horndeski, Int. J. Theor. Phys. **10**, 363-384 (1974).
[23] C. Deffayet, X. Gao, D. A. Steer and G. Zahariade, Phys. Rev. D **84**, 064039 (2011) [arXiv:1103.3260 [hep-th]].
[24] T. Kobayashi, M. Yamaguchi and J. 'i. Yokoyama, Prog. Theor. Phys. **126**, 511 (2011) [arXiv:1105.5723 [hep-th]].
[25] C. Charmousis, E. J. Copeland, A. Padilla and P. M. Saffin, Phys. Rev. Lett. **108**, 051101 (2012) [arXiv:1106.2000 [hep-th]].
[26] C. de Rham, G. Gabadadze, L. Heisenberg and D. Pirtskhalava, Phys. Rev. D **83**, 103516 (2011) [arXiv:1010.1780 [hep-th]].
[27] C. Burrage, C. de Rham, L. Heisenberg and A. J. Tolley, JCAP **1207**, 004 (2012) [arXiv:1111.5549 [hep-th]].
[28] C. de Rham and L. Heisenberg, Phys. Rev. D **84**, 043503 (2011) [arXiv:1106.3312 [hep-th]].
[29] L. Heisenberg, R. Kimura and K. Yamamoto, Phys. Rev. D **89**, 103008 (2014) [arXiv:1403.2049 [hep-th]].
[30] M. Zumalacarregui and J. Garcia-Bellido, Phys. Rev. D **89**, 064046 (2014) [arXiv:1308.4685 [gr-qc]].
[31] J. Gleyzes, D. Langlois, F. Piazza and F. Vernizzi, Phys. Rev. Lett. **114**, 21, 211101 (2015) [arXiv:1404.6495 [hep-th]].
[32] D. Langlois and K. Noui, JCAP **1602**, no. 02, 034 (2016) [arXiv:1510.06930 [gr-qc]].
[33] J. Beltran Jimenez and T. S. Koivisto, Phys. Lett. B **756**, 400 (2016) [arXiv:1509.02476 [gr-qc]].
[34] J. Beltran Jimenez, L. Heisenberg and T. S. Koivisto, JCAP **1604**, 046 (2016) [arXiv:1602.07287 [hep-th]].
[35] L. Heisenberg, JCAP **1405**, 015 (2014) [arXiv:1402.7026 [hep-th]].
[36] G. Tasinato, JHEP **1404**, 067 (2014) [arXiv:1402.6450 [hep-th]].
[37] E. Allys, P. Peter and Y. Rodriguez, JCAP **1602**, no. 02, 004 (2016) [arXiv:1511.03101 [hep-th]].
[38] J. Beltran Jimenez and L. Heisenberg, Phys. Lett. B **757**, 405 (2016) [arXiv:1602.03410 [hep-th]].
[39] L. Heisenberg, R. Kase and S. Tsujikawa, Phys. Lett. B **760**, 617 (2016) [arXiv:1605.05565 [hep-th]].
[40] R. Kimura, A. Naruko and D. Yoshida, JCAP **1701**, 002 (2017) [arXiv:1608.07066 [gr-qc]].
[41] A. De Felice, L. Heisenberg, R. Kase, S. Mukohyama, S. Tsujikawa and Y. l. Zhang, JCAP **1606**, 048 (2016) [arXiv:1603.05806 [gr-qc]].
[42] A. De Felice, L. Heisenberg, R. Kase, S. Mukohyama, S. Tsujikawa and Y. l. Zhang, Phys. Rev. D **94**, no. 4, 044024 (2016) [arXiv:1605.05066 [gr-qc]].
[43] A. De Felice, L. Heisenberg, R. Kase, S. Mukohyama, S. Tsujikawa and Y. l. Zhang, Phys. Rev. D **94**, 044024 (2016) [arXiv:1605.05066 [gr-qc]].
[44] J. Beltran Jimenez and L. Heisenberg, Phys. Lett. B **770**, 16 (2017) [arXiv:1610.08960 [hep-th]].
[45] R. Emami, S. Mukohyama, R. Namba and Y. l. Zhang, JCAP **1703**, 058 (2017) doi:10.1088/1475-7516/2017/03/058 [arXiv:1612.09581 [hep-th]].
[46] J. Beltran Jimenez, R. Durrer, L. Heisenberg and M. Thorsrud, JCAP **1310**, 064 (2013) [arXiv:1308.1867 [hep-th]].
[47] J. Beltran Jimenez, L. Heisenberg, R. Kase, R. Namba and S. Tsujikawa, Phys. Rev. D **95**, no. 6, 063533 (2017) [arXiv:1702.01193 [hep-th]].
[48] M. Hull, K. Koyama and G. Tasinato, JHEP **1503**, 154 (2015) [arXiv:1408.6871 [hep-th]].
[49] M. Hull, K. Koyama and G. Tasinato, Phys. Rev. D **93**, 064012 (2016) [arXiv:1510.07029 [hep-th]].
[50] E. Allys, P. Peter and Y. Rodriguez, Phys. Rev. D **94**, no. 8, 084041 (2016) [arXiv:1609.05870 [hep-th]].
[51] G. W. Horndeski, J. Math. Phys. **17**, 1980 (1976).
[52] B. F. Schutz and R. Sorkin, Annals Phys. **107**, 1 (1977).
[53] B. Boisseau, G. Esposito-Farese, D. Polarski and A. A. Starobinsky, Phys. Rev. Lett. **85**, 2236 (2000) [gr-qc/0001066].
[54] S. Tsujikawa, Phys. Rev. D **76**, 023514 (2007) [arXiv:0705.1032 [astro-ph]].
[55] A. De Felice, T. Kobayashi and S. Tsujikawa, Phys. Lett. B **706**, 123 (2011) [arXiv:1108.4242 [gr-qc]].
[56] L. Amendola, M. Kunz and D. Sapone, JCAP **0804**, 013 (2008) [arXiv:0704.2421 [astro-ph]].
[57] Y. Wang and P. Mukherjee, Phys. Rev. D **76**, 103533 (2007) [astro-ph/0703780].
[58] E. Komatsu *et al.* [WMAP Collaboration], Astrophys. J. Suppl. **180**, 330 (2009) [arXiv:0803.0547 [astro-ph]].
[59] Y. Wang and S. Wang, Phys. Rev. D **88**, 043522 (2013) [arXiv:1304.4514 [astro-ph.CO]].
[60] W. Hu and N. Sugiyama, Astrophys. J. **444**, 489 (1995) [astro-ph/9407093].
[61] Y. Wang and M. Dai, Phys. Rev. D **94**, no. 8, 083521 (2016) [arXiv:1509.02198 [astro-ph.CO]].
[62] P. A. R. Ade *et al.* [Planck Collaboration], Astron. Astrophys. **594**, A14 (2016) [arXiv:1502.01590 [astro-ph.CO]].
[63] D. J. Eisenstein and W. Hu, Astrophys. J. **496**, 605 (1998) [astro-ph/9709112].
[64] D. J. Eisenstein *et al.* [SDSS Collaboration], Astrophys. J. **633**, 560 (2005) [astro-ph/0501171].
[65] F. Beutler *et al.*, Mon. Not. Roy. Astron. Soc. **423**, 3430 (2012) [arXiv:1204.4725 [astro-ph.CO]].
[66] A. J. Ross, L. Samushia, C. Howlett, W. J. Percival, A. Burden and M. Manera, Mon. Not. Roy. Astron. Soc. **449**, no. 1, 835 (2015) [arXiv:1409.3242 [astro-ph.CO]].
[67] S. Alam *et al.* [BOSS Collaboration], arXiv:1607.03155 [astro-ph.CO].
[68] L. Anderson *et al.* [BOSS Collaboration], Mon. Not. Roy. Astron. Soc. **441**, no. 1, 24 (2014) [arXiv:1312.4877 [astro-ph.CO]].
[69] E. A. Kazin *et al.*, Mon. Not. Roy. Astron. Soc. **441**, no. 4, 3524 (2014) [arXiv:1401.0358 [astro-ph.CO]].
[70] A. G. Riess *et al.* [Supernova Search Team], Astron. J. **116**, 1009 (1998) [astro-ph/9805201].
[71] S. Perlmutter *et al.* [Supernova Cosmology Project Collaboration], Astrophys. J. **517**, 565 (1999) [astro-ph/9812133].

[72] N. Suzuki *et al.*, Astrophys. J. **746**, 85 (2012) [arXiv:1105.3470 [astro-ph.CO]].
[73] A. G. Riess *et al.*, Astrophys. J. **826**, no. 1, 56 (2016) [arXiv:1604.01424 [astro-ph.CO]].
[74] A. De Felice and S. Mukohyama, Phys. Rev. Lett. **118**, 091104 (2017) [arXiv:1607.03368 [astro-ph.CO]].
[75] T. Okumura *et al.*, Publ. Astron. Soc. Jap. **68**, no. 3, 38, 24 (2016) [arXiv:1511.08083 [astro-ph.CO]].
[76] A. De Felice and S. Tsujikawa, JCAP **1202**, 007 (2012) [arXiv:1110.3878 [gr-qc]].
[77] A. De Felice and S. Tsujikawa, JCAP **1203**, 025 (2012) [arXiv:1112.1774 [astro-ph.CO]].
[78] P. A. R. Ade *et al.* [Planck Collaboration], Astron. Astrophys. **594**, A13 (2016) [arXiv:1502.01589 [astro-ph.CO]].
[79] G. D. Moore and A. E. Nelson, JHEP **0109**, 023 (2001) [hep-ph/0106220].
[80] R. Kimura and K. Yamamoto, JCAP **1207**, 050 (2012) [arXiv:1112.4284 [astro-ph.CO]].
[81] S. Nakamura, R. Kase and S. Tsujikawa, Phys. Rev. D **95**, 104001 (2017) [arXiv:1702.08610 [gr-qc]].